Factors regulating primary producers' assemblages in *Posidonia oceanica* (L.) Delile ecosystems over the past 1800 years.

Carmen Leiva-Dueñas[1]*, Peter R. Leavitt[2,3], Teresa Buchaca[1]., Antonio Martínez Cortizas[4, 1], Lourdes López-Merino[4], Oscar Serrano[5], Paul S. Lavery,[1, 5], Stefan Schouten[6, 7], Miguel A. Mateo[1,5]

[1] Centro de Estudios Avanzados de Blanes, Consejo Superior de Investigaciones Científicas, Blanes, Spain

[2] Institute of Environmental Change and Society, University of Regina, Regina, Canada

[3] Institute for Global Food Security, Queen's University Belfast, Belfast, United Kingdom

[4] EcoPast (GI-1553), Facultade de Bioloxía, Universidade de Santiago de Compostela, Santiago de Compostela, Spain

[5] School of Natural Sciences and Centre for Marine Ecosystems Research, Edith Cowan University, Joondalup, Australia

[6] Department of Marine Biogeochemistry and Toxicology, Royal Netherlands Institute for Sea Research, Texel, the Netherlands

[7] Department of Geosciences, Utrecht University, Utrecht, the Netherlands.

* **Corresponding author:** C. Leiva-Dueñas; e-mail: cleiva@ceab.csic.es; carmenld92@hotmail.com; telephone: +34 972 33 61 01; Full postal address: Centro de Estudios Avanzados de Blanes, Consejo Superior de Investigaciones Científicas, Carrer Accés Cala Sant Francesc, 14, 17300, Blanes, Spain

Abstract

Posidonia oceanica (L.) Delile meadows are highly productive coastal marine ecosystems that provide multiple ecosystem services. The seagrass is not always the major contributor to total primary production, however, little is known about long-term changes in the composition of primary producers within seagrass meadows. Understanding compositional shifts within the community of primary producers is crucial to evaluate how climate and anthropogenic change affect the functioning of seagrass ecosystems. Here we analysed marker pigment composition in seagrass cores from two bays of the Cabrera Island (Balearic Islands, Spain) to asses long-term changes in phototrophic community composition and production in seagrass meadows, and identify the environmental factors triggering those changes. The proxy dataset was explored using principal component analyses (PCA): one including the pigment dataset to look for associations between producers' groups, and another one combining the pigment dataset with plausible local and global regulatory factors to assess the environmental drivers of change. Analyses of characteristic pigments and morphological fossils (cysts) showed that the abundance of dinoflagellates increased over the last 150-300 years, coeval with a rise in solar irradiance and air temperature. When compared among embayments, pigments from cyanobacteria predominated in seagrass meadows located at Es Port, a sheltered bay receiving higher terrestrial runoff; whereas pigments from diatoms, seagrasses and rodophytes were more common at Santa Maria, an exposed bay with clearer waters. Water depth also played a role in controlling the phototrophic community composition, with greater abundance of diatoms in the shallowest waters (< 5 m). Overall, our results suggested that historical and spatial variation in seagrass meadows' phototrophic community composition was influenced by the interaction between local factors (catchment-bay characteristics) and global climate processes (energy influx). Together these patterns forecast how marine primary producers and seagrass ecosystem structure may respond to future global warming.

Keywords: Late Holocene; Western Mediterranean; seagrass; primary producers' composition; fossil pigments; climate change.

1. Introduction

Posidonia oceanica seagrass meadows are one of the most valuable habitats in the Mediterranean Sea owing to their multiple ecosystem services (Spalding et al., 2003). However, this endemic species has exhibited widespread decline since the early 20th century, mainly due to local anthropogenic pressures such as coastal development, pollution, trawling, fish farming, moorings, dredging, dumping and introduced species (Boudouresque et al., 2009). Fortunately, de los Santos et al. (2019) showed that seagrass loss rates recently slowed down due to effective conservation and restoration actions, including habitat protection. Despite this promising news, relatively little is known about how *P. oceanica* meadows have varied historically in response to perturbations.

Therefore, elucidation of the long-term dynamics and environmental drivers of ecosystem change is required to evaluate the magnitude of current declines in an historical context, as well as to predict, prevent or mitigate the effects of present and future environmental changes on seagrass meadows structure and function (López-Merino et al., 2017; Leiva-Dueñas et al., 2018).

Total primary production of seagrass ecosystems does not always depend on the seagrass species as the major contributor. Other primary producers inhabiting the meadows can contribute substantially (up to 60% of total production), including epiphytes, phytoplankton, phytobenthos and macroalgae (McRoy & McMillan, 1977; Borowitzka et al., 2006; Mateo et al., 2006). The abundance and composition of primary producers' communities within seagrass meadows are regulated by complex mechanisms reflecting interactions between physico-chemical (e.g., light, temperature, water movement, nutrients) and biological factors (e.g., competition for space, grazing and predation) (Koch, 2001; Borowitzka et al., 2006) (Fig. 1). Regulation of composition at the decadal-scale appears to mainly involve competition for light and nutrients between micro- and macroalgae and the seagrass (Delgado et al., 1999; Hemminga & Duarte, 2000; Ralph et al., 2006). Elevated nutrient concentrations favour phytoplankton blooms, as well as epiphyte and macroalgae overgrowth, all leading to attenuation of irradiance and diminished transmission to the seagrass canopy (McGlathery et al., 2007; Viaroli et al., 2008) (Fig. 1).

Epiphyte composition in seagrass leaves is influenced by complex interactions between nutrients, light, temperature, water motion, salinity, and seagrass physiological and phenological characteristics, as well as the biotic interactions between epiphytes, herbivores and predators (Armitage et al., 2006; Lavery et al., 2007; Prado et al., 2007; Mabrouk et al., 2014). In addition, epiphyte assemblages often vary predictably along a depth gradient due to changes in light, local hydrodynamics, and meadow structure (Borowitzka et al., 2006; Tsirika et al., 2007; Nesti et al., 2090; Piazzi et al., 2016) (Fig. 1).

Research on the factors regulating the complex interactions influencing coastal marine ecosystem production and composition over centennial timescales lags behind that of lacustrine and terrestrial habitats, mainly because of the relative scarcity of reliable coastal marine archives owing to their hydrodynamism (Hay, 1974; Mateo et al., 2010). *P. oceanica* meadows are an exception, since coherent sequences with high temporal resolution (2-17 yr cm^{-1}) can be obtained in them (Serrano et al., 2012; Serrano et al., 2016a). These *Posidonia* environmental archives, known as mats, consist of large pools of organic matter accumulated over millennia, mainly as decay-resistant plant debris and organic or inorganic remains of other meadow-inhabiting organisms (Mateo et al., 1997; Lo Iacono et al., 2008; Kaal et al., 2016). Therefore, mats can potentially preserve a wide range of biotic and abiotic proxies due to the prevailing anoxic conditions (Mateo et al., 2006; Piñeiro Juncal et al., 2018).

Proxy analyses on *Posidonia* mats allow quantification of diverse long-term environmental and ecological changes as, for example, the impact of land-use change and metal pollution on coastal systems, the role of climatic factors and seagrass revegetation in carbon burial, and historical variation in seagrass productivity (López-Sáez et al., 2009; Mateo et al., 2010; Serrano et al., 2011, 2013, 2016b, 2016c; Macreadie et al., 2015; Marba et al., 2015; López-Merino et al., 2015, 2017; Leiva-Dueñas et al., 2018). To date, however, fossils pigments from phototrophic organisms have not been used to quantify long-term changes in the production or gross community composition of seagrass systems, unlike studies on some other marine systems (Kowalewska et al., 2004; Rabalais et al., 2004; Reuss et al., 2005, 2010).

Aiming at filling the abovementioned knowledge gap, we measured past changes in concentrations of fossil pigments from diverse phototrophic organisms, in combination with other proxies (e.g., sedimentological, geochemical and dinoflagellate cysts), in five *P. oceanica* mat cores from two bays of the Cabrera National Park, Balearic Islands, Spain. The objectives of this study were: (1) to measure the variability in pigment composition through time and across spatial gradients (water depth within a bay) in two bays with contrasting features, and; (2) to identify the long-term environmental drivers which may regulate the phototrophic community composition in the meadows.

2. Material and methods

2.1. Environmental setting and coring procedures

The Cabrera Island is the largest island of the Cabrera Archipelago, located south of Mallorca (Balearic Islands) in the western Mediterranean Sea (Fig. 2). The climate of the island is semi-arid and although precipitation is scarce, there are several small watersheds that are active only during intense precipitation periods (Alcover et al., 1993). The main watershed drains into Es Port Bay (Rodríguez-Perea & Servera, 1993). The surrounding coastal waters are warm with very low nutrient content comparing to other coastal Mediterranean waters (Ballesteros & Zabala, 1993).

Five *P. oceanica* mat cores were taken in June 2015 from meadows growing in two bays: Santa Maria (SM), and Es Port (EP) (Fig. 2). Cores were collected at a single station 5-m below the sea level (bsl) at EP and along a depth-transect (5, 10, 15, and 25 m bsl) at SM (Table 1). SM is a relatively exposed bay with an area of 1.14 km^2 (55 m maximum depth) connected to the open sea by a 1.2-km wide mouth. On the contrary, EP (0.8 km^2, 45 m maximum depth) forms a relatively sheltered environment with a narrower opening (650 m) (Fig. 2). Cores were collected by scuba divers using high-density PVC pipes fitted with core catchers and a serrated leading edge. Exponential decompression functions were applied to correct for core shortening (Morton & White, 1997; Serrano et al., 2012).

At both bays, *P. oceanica* grows on biogenic, carbonate-rich and iron-deficient sediments (Holmer et al., 2005; Marbà et al., 2008). About 42% of SM benthos is covered by dense, continuous *P. oceanica* meadows, whereas meadows in EP cover less area (36%) and occur at shallower depth (Marbà et al., 2002). Demographic analysis indicates that while meadows at SM are in good condition, those at EP exhibit symptoms of stress, including lower leaf production rates and vertical rhizome elongation, very low shoot recruitment, higher mortality, and elevated sulphate reduction rates. The different seagrass conditions between bays have been attributed to contrasting water residence times in EP (7-15 days) and SM (4 days) (Marbà et al., 2002; Orfila et al., 1992, 2005), and to more frequent and intensive anthropogenic activities at EP (Marbà et al., 2002).

2.2. Sedimentology, geochemical analyses and core chronology

Cores were cut longitudinally and opened into two halves. One-half was analysed non-destructively for elemental composition using X-ray fluorescence (XRF) with an AVAATECH core scanner at the CORELAB laboratory, University of Barcelona. One cm-thick samples from one of the half-cores were dried at 60ºC until constant weight to determine dry bulk density, then homogenized using an automated agate mortar (Mortar Grinder RM-200 RETSCH).

Organic matter content (OM) was estimated in the samples by mass-loss-on-ignition at 550º for 4h. Sediment grain size was determined using a laser-diffraction particle analyser (Mastersizer 2000, Malvern instruments Ltd., UK). Carbon and N elemental and isotopic composition of sediment samples were analysed at UH Hilo Analytical Laboratory, University of Hawaii at Hilo, on a Thermo-Finnegan Delta V IRMS isotope ratio mass spectrometer coupled with a Costech elemental analyser.

Isoprenoid glycerol dialkyl glycerol tetraether (GDGT) lipids were used to calculate the Branched and Isoprenoid Tetraether (BIT) index, an index of the relative abundance of terrestrial and autochthonous organic matter in marine sediments (Hopmans et al., 2004). The samples polar fraction were analysed for GDGTs according to Schouten et al. (2007). GDGT analyses were performed using liquid chromatography–mass spectrometry (LC–MS) with a Hewlett Packard1100 Series instrument equipped with an auto-injector and ChemStation chromatography manager software.

Radiocarbon (^{14}C) and lead-210 (^{210}Pb) activities were measured using accelerator mass spectrometry (DirectAMS laboratory) and alpha spectrometry (Environmental Radioactivity Laboratory, Autonomous University of Barcelona), respectively, to obtain age-depth models for the collected cores.

Raw proxy data trends are presented in Fig. S1.

2.3. Fossil pigment analysis

Pigments and their derivatives were extracted, isolated, identified and quantified using high-performance liquid chromatography (HPLC) with an Agilent model 1100 instrument at University of Regina following standard methods of Leavitt & Hodgson (2001). Fossil pigment interpretations were restricted to a subset of carotenoid and chlorophyll biomarkers that commonly preserve in sedimentary deposits (Table 3). Predominant phorbins identified included metrics of total primary producers such as labile Chlorophyll-*a* (chl-*a*; a precursor), pheophytin *a* (Chl's stable product), and chlorophyte markers (chl-*b*, pheophytin *b*). Pigment preservation index (PPI) was calculated from the ratio of chl-*a* to its degradation product pheophytin *a*. Complete fossil pigment profiles are presented in Fig. S2.

2.4. Organic-walled dinoflagellate cysts analysis

A palynological analysis of pollen and non-pollen palynomorphs (NPP) of the cores is currently under way. Among the NPP, we have identified organic-walled dinoflagellate cysts (dinocysts); microremains relevant for this study due to their relationship with some of the analysed pigments. The results from core EP05 and the preliminary results from core SM25 are presented herein. Pollen and NPP were isolated from seagrass deposits using standard palynological extraction protocols, including sediment digestion with HCl, NaOH and HF to eliminate carbonates, humic acids and silicates, respectively (Fægri & Iversen, 1989). Dinocysts were identified and counted using light microscopy at ×400 magnifications.

2.5. Numerical procedures

Principal component analysis (PCA) was used to explore potential associations in the community of primary producers as recorded by fossil pigment concentrations in the cores ($PCA_{pigments}$). Fossil pigment data were reported in units of concentration and, as such, are compositional data which required isometric log-ratio transformation prior the analysis (Aitchison, 1986; Egozcue et al., 2003; Filzmoser et al., 2010). The analysis consisted in a robust PCA via *pcaCoDa* command in "*robcompositions*" package in the R computational environment (Templ et al., 2011).

To determine which environmental variables were the most influential on pigment marker composition, another robust PCA was run including both local factors and global climate indicators ($PCA_{environmental}$). Local factors included biotic variables such as total primary production (as chl-*a*, β-carotene and OM), nutrient cycling and organic matter supply (C and N stable isotope values and BIT index), as well as abiotic descriptors (sediment grain size, and C and N elemental composition, XRF-measured elements). Global climate external factors included indices of Total Solar Irradiance (TSI, Vieira et al., 2011), Northern Hemisphere Temperature (NHT, Kobashi et al., 2013) and the North Atlantic Oscillation (NAO; Hurrell, 2003; Trouet et al., 2009; Olsen et al., 2012) - NAO is an atmospheric mode affecting the hydrological variability in the western Mediterranean (Roberts et al., 2012).

Generalized additive models (GAMs) were used to estimate temporal trends in the principal components scores and dinocyst concentrations. GAMs are able to model non-linear relationships between time and a response variable and can handle the irregular spacing typical in palaeoecological time series (Simpson, 2018). Thin-plate regression splines were used to parametrise the smooth functions of time (Wood, 2003). The differences between the fitted smooth functions for $PC1_{pigments}$ scores and concentrations of dinocysts were calculated as in Rose et al. (2012). GAMs were performed using the mgcv package in R (Wood, 2004, 2016, 2017).

All statistical analyses were conducted using R statistical software (R Core Team, 2018) and detailed descriptions of the materials and methods section are given in Supplementary Material.

3. Results

3.1. Age-depth models

The age-depth models combining radiocarbon and ^{210}Pb dates revealed that core SM15 extended back to ~1900 cal. yr BP, whereas cores SM25 and EP05 extended to ~1700 cal. yr BP (Table 2, Fig. 3A). Cores SM05 and SM10 encompassed less time, SM05 dated back to ~100 and SM10 to ~700 cal. yr BP. Overall, accumulation rates varied between 0.02 and 2 cm/yr with significantly differences among cores (median Kruskal-Wallis test, $p<0.05$). A nonparametric pairwise multiple comparison (Dunn's test, $p<0.05$) confirmed all median rates were significantly different with the exception of the pair EP05 - SM15 ($p=0.754$). Accumulation rates decreased with increasing water depth in SM, from a median of 0.36 cm/yr (SM05) to a median of 0.06 cm/yr (SM25) (Fig. 3B). In most cores, mat accumulation was likely continuous with the exception of EP05 which exhibited an apparent hiatus between ~ 300 and ~1250 cal. yr BP - based on a large jump of ~950 calibrated years between two radiocarbon dates at 60 and 64 cm depth in the core (Fig. 3A and Table 2).

3.2. Primary producers' composition

Trends in the pigment composition within all cores were well described using a robust PCA with two principal axes, explaining 91% of the total variance (Fig. 4A). The first principal component ($PC1_{pigments}$, 78%) showed a high positive loading for diadinoxanthin (dinoflagellates, diatoms and chrysophytes) and moderate negative loadings for echinenone (total cyanobacteria), lutein-zeaxanthin (chlorophytes, higher plants, rhodophytes and cyanobacteria) and canthaxanthin (Nostocales –cyanobacteria–) (Fig. 4A and Table 4). The second principal component ($PC2_{pigments}$, 13%) showed high positive loadings for diatoxanthin (mainly diatoms) and lutein-zeaxanthin (chlorophytes, higher plants, cyanobacteria and rhodophytes), and high-to-moderate negative loadings for echinenone (total cyanobacteria) and canthaxanthin (Nostocales –cyanobacteria–) (Fig. 4A and Table 5).

The main temporal trend observed in all cores was an increase in $PC1_{pigments}$ scores towards the present, particularly during the last ~150-300 years. This trend mainly reflects increasing concentrations of diadinoxanthin (Fig. 4B). Sample scores from $PC2_{pigments}$ did not show a consistent change through time, although they did show an evident spatial pattern, with different pigment composition between bays (Fig. 4). Higher proportions of diatoxanthin and lutein-zeaxanthin were found in SM, while canthaxanthin and echinenone predominated in EP. Within SM, sample scores indicated a greater abundance of diatoxanthin and lutein-zeaxanthin in the shallowest area (SM05) of the bay (Fig. 4B).

3.3. Relationship between fossil pigment composition and environmental factors

A robust PCA explained 57% of the variance in fossil pigment composition using a combination of local and global predictive variables (Fig. 5A and Table 5). The first axis ($PC1_{environmental}$) accounted for 31% of the total variance and showed that diadinoxanthin was strongly and positively correlated with global climate indicators (TSI and NHT). Diadinoxanthin content was also moderately and positively correlated to $\delta^{13}C$, concentrations of chl-*a*, and the PPI. Echinenone and lutein-zeaxanthin abundances were also correlated moderately and negatively with diadinoxanthin (Fig. 5A).

$PC2_{environmental}$ accounted for 26% of the total variation (Fig. 5A). On this axis, abundances of diatoxanthin and lutein-zeaxanthin were positively correlated with chlorine, medium and fine-sands, PPI and chl-*a* content, while negatively correlated with echinenone and canthaxanthin. In contrast, echinenone and canthaxanthin were positively correlated with OM, $\delta^{15}N$, the BIT index, coarse-sandy fractions and β-carotene, and negatively with diatoxanthin and lutein-zeaxanthin (Fig. 5A and Table 5).

Overall, $PC1_{environmental}$ scores exhibited an increasing trend towards the present in most cores, in particular during the last 150-300 years (Fig. 5B). Temporal trends of $PC2_{environmental}$ scores showed no clear nor common pattern among cores through time, although they did show the same difference among embayments as described for $PC2_{pigments}$ (Fig. 5B).

3.4. Dinocyst records

Dinocysts concentrations were low in sediments from both bays. They were 1-2 orders of magnitude higher in EP05 than in SM25 (Fig. 6). All dinocysts identified were of autotrophic affinity. In both bays, dinocyst concentrations were composed predominately of *Spiniferites* spp. and *Lingulodinium machaerophorum*. *L.*

machaerophorum is the cyst produced by the motile form *Lingulodinium polyedrum*, a species which inhabits estuaries and coastal bays worldwide, including the Mediterranean Sea (Lewis & Hallett, 1997; Penna et al., 2006). The most notable feature of the dinocyst records is the presence of a trend towards increasing concentrations during the last two centuries, particularly for *Spiniferites* spp., *L. machaerophorum*, *Operculodinium* spp., and for total dinocysts (Fig. 6). These trends were significant only for EP05, which is perhaps related to the larger amount of samples processed in EP05 compared to SM25.

GAMs were employed to test if the temporal changes in concentrations of dinoflagellate pigment diadinoxanthin (as $PC1_{pigments}$ scores) were similar to those recorded for dinocysts (Fig. 7). Here the differences between the GAM-fitted pigments and cyst trends were estimated only for the most recent 250 yrs, the period during which there was directional change in fossil abundance in EP05. Comparisons were conducted between $PC1_{pigments}$ and total cyst concentrations (TC), as well as between $PC1_{pigments}$ and cysts from *Lingulodinium machaerophorum* (LM) and *Spiniferites* spp. (SS). Confidence intervals not encompassing zero, are indicative of significant differences between the smoothed trends (Rose et al., 2012). In EP05 core, no difference was observed between trends in any metric of cyst abundance (TC, LM or SS) and PC1 scores during the last 250 years (Fig. 7). Therefore, we infer that the increasing recent trend in $PC1_{pigment}$ and by inference the dinoflagellate biomarker diadinoxanthin mainly reflect changes in fossil concentrations of dinoflagellate cysts at least in the EP05 core (Fig. 6 and 7).

4. Discussion

4.1. Seagrass phototrophic community

The overall composition of sedimentary pigments from the mat cores was consistent with the expected assemblage of primary producers observed in *P. oceanica* meadows. In general, modern macroalgal species are characteristically composed mainly of calcareous Rhodophyta and non-calcified Ochrophyta, whereas microalgal epiphytes usually include diatoms, dinoflagellates and cyanobacteria in declining relative abundance (Piazzi et al., 2016; Agawin et al., 2017). Similarly, the modern phytoplankton assemblages are mainly composed of diatoms and dinoflagellates (Moncer et al., 2017), while the water column near Cabrera is known to harbour a great abundance of pico and nanoplankton, dinoflagellates, coccolitophorids and diatoms (Vives, 1993). We suggest that seagrass, possibly in association with rhodophytes, is the main source of the couplet lutein-zeaxanthin, as it is the most abundant carotenoid in live *P. oceanica* tissues (Casazza & Mazella, 2002).

4.2. Observed temporal and spatial patterns

Multivariate analysis of the cores revealed two main patterns of change in the fossil pigment assemblages. First, we recorded a temporal shift in the abundance of dinoflagellates and siliceous algae, which appears to reflect the influence of global climate change, particularly the inputs of energy as irradiance and heat (i.e., TSI and NHT). Second, our results showed clear spatial patterns in primary producers' community composition, seemingly related to embayment-specific local conditions (EP *versus* SM), and to the water depth gradient (SM gradient). Taken together, these patterns suggest that primary producers in seagrass meadows are influenced by a combination of global and local regulatory mechanisms.

4.2.1. The recent increase in dinoflagellates

Increased abundance of dinoflagellates and possibly siliceous taxa (as the carotenoid diadinoxanthin) was observed among all cores over the last 150-300 years (Fig. 4 and 5). Our results suggest that the carotenoid diadinoxanthin was more abundant during episodes of high solar irradiance (i.e., TSI), air temperature (i.e., NHT) and, to a lesser extent, ecosystem production (i.e., $\delta^{13}C$ and chl-*a*) according to $PC1_{environmental}$ (Fig.5A). Hence, changes in dinoflagellate abundance seem to be influenced by global climate variables - specifically the input of energy as irradiance and heat. Changes in pigment preservation may also partly explain these historical trends, as noted with the direction of the pigment preservation index vector (Fig. 5A). Post-depositional degradation may contribute to the decline in labile diadinoxanthin with increasing sediment age ($PC1_{pigments}$ and $PC1_{environmental}$, Fig. 4B and 5B). However, analysis of resting cysts from dinoflagellates in cores EP05 and SM25 also showed an increase in dinoflagellate abundance over the same period, especially for *L. machaerophorum* and *Spiniferites* spp. in EP05 (Fig. 6). Dinocysts are composed of highly resistant organic compounds, which are preserved well in sediments (Versteegh & Blokker, 2004). Given the strong concordance between historical trends in the dinoflagellate biomarker diadinoxanthin (as $PC1_{pigments}$) and dinoflagellate cyst concentrations, we infer that increased abundance of diadinoxanthin over the past ~250 years reflects actual changes in algal biomass, rather than slow post-depositional degradation in the *Posidonia* seagrass mats.

The observed orthogonal relationship between diadinoxanthin and diatoxathin in the two PCAs was unexpected because both pigments usually co-occur in several algal groups, as in diatoms and dinoflagellates. Although speculative, this lack of correlation could be due to the fact that they are associated with different algal groups in the particular setting of Cabrera: diadinoxanthin with dinoflagellates and diatoxanthin with diatoms. Regardless, the uncorrelated nature of historical trends in diadinoxanthin and the diatom-specific biomarker diatoxanthin again suggests that historical trends in diadinoxanthin were recording mainly changes in marine dinoflagellate abundance.

Increased abundance of dinoflagellates during periods of elevated solar irradiance may be related to their ability to produce substantial amounts of UV-absorbing photo-protective compounds under high irradiance (Hannach & Sigleo, 1998). In this sense, diadinoxanthin is known to act as a photoprotective accessory pigment (Lavaud et al., 2002; Laviale & Jacques, 2011). Diadinoxanthin is not only present in dinoflagellates but also in some species of raphidophytes (e.g., *Heterosigma akashiwo, Chattonella subsalsa),* which also thrive in high UV environments (Fu et al., 2012; Wells et al., 2015). Similarly, elevated water temperature may favour growth of epiphytic dinoflagellates and diatoms in seagrass meadows (Johnson et al. , 2005; Turki, 2005; Frankovich et al., 2006; Mabrouk et al., 2012). Moreover, the correlation between dinoflagellates and temperature found here was also described in several long-term dinocyst records, in which high *L. machaerophorum* and *Spiniferites* spp. abundance correlated with warmer sea surface waters and stronger stratified conditions in coastal areas (Pospelova et al., 2006; Sobrino et al., 2012; Bringué et al., 2013; Leroy et al., 2013). Those studies also reported sharp increases in *L. machaerophorum* over the last century, similar to the patterns observed in this study (Fig. 5A). *L. machaerophorum* is also a potentially-toxic taxon, known to produce yessotoxins (e.g. Paz et al., 2004; Armstrong & Kudela, 2006). Therefore, their higher abundance could increase the risk of toxic algal blooms that could affect the entire ecosystem composition and structure (Sellner et al., 2003).

Our results provide a predictive understanding of the response of phototrophic assemblages in seagrass meadows to global change. Specifically, we anticipate an increase in dinoflagellates as a consequence of global warming. The exact consequences of this change in the composition of primary producers are so far unknown. Our study points to a greater contribution of autotrophic dinoflagellates to autotrophic production in seagrass meadows, possibly leading to the outcompetition of the seagrass (Fig. 5A). Providing dinoflagellates do not outcompete the seagrass and go through mass encystment, they could even have an effective contribution to carbon sequestration (Spilling et al., 2014; Wasmund et al., 2017). However, the latter speculation may be difficult to evaluate, as *P. oceanica* is thought to be negatively impacted by the on-going sea water warming (Marba & Duarte, 2010; Savva et al., 2018).

4.2.2. Spatial differences between bays and along water depth

Our results revealed pronounced spatial patterns in primary producer community composition, caused by site-specific local effects, as well as the natural depth gradient. In the anthropogenically-impacted EP setting, the community was mainly dominated by cyanobacteria (as canthaxanthin and echinenone), whereas diatoms (as diatoxanthin), chlorophytes, rhodophytes and, most probably, the seagrass (all as lutein-zeaxanthin) were more characteristic of the less disturbed SM setting. As detailed below, these patterns may arise because of basin-specific differences in local land use and catchment characteristics, specifically nutrient and terrestrial organic matter inputs.

The cyanobacteria-rich community of EP developed in an environment with elevated organic matter and nutrient inputs, mainly of terrestrial origin (high loadings for BIT index, δ^{15}N and OM in PC2 $_{\text{environmental}}$, Fig. 5). In EP, higher microbial decay would also explain the δ^{15}N enriched sediment organic matter relative to that of SM (Craine et al., 2015). Aside from high nutrient availability, EP waters have other physical conditions favourable to elevated cyanobacterial abundance compared to SM, such as longer water residence times and enhanced stratification (Orfila et al., 2005;

Paerl & Huisman, 2008). On the other hand, diatoms, the seagrass and likely, rodophytes prevailed in SM (Fig. 4A), where organic matter is mainly derived from marine autochthonous production, as indicated by a high loading for chlorine in $PC2_{environmental}$ (Fig. 5A), an element known to be incorporated in labile marine organic matter (Leri et al., 2015). Our findings support those of Holmer et al. (2003, 2004) who reported an organic enrichment and higher mineralization rates in EP, as well as a significantly higher net community production in SM, reflecting higher light availability, lower terrestrial inputs and higher water turnover rates.

Studies of phytoplankton communities in marine waters have observed increases in the abundance of cyanobacteria under ammonium enrichment, whereas diatoms more commonly bloom when exposed to elevated nitrate concentrations (Berg et al., 2003; Heil et al., 2007; Glibert et al., 2014). Cyanobacteria are generally considered specialists that have a superior ammonium uptake kinetics (Blomqvist et al., 1994; Lindell & Post, 2001). Further, cyanobacteria can use organic matter as a nitrogen source in both lakes and marine ecosystems (e.g., Berman, 2001; Sakamoto & Bryant, 2001; Berg et al., 2003; Glibert et al., 2004; Donald et al., 2011). Therefore, the predominance of cyanobacteria in EP could reflect an elevated influx of ammonium or other N species as a result of the enhanced organic matter decomposition in this bay (Holmer et al., 2004; Pérez et al., 2007), or higher availability of dissolved organic matter. The naturally high organic matter accumulation in EP arises from discharges of the main pluvial network of the island (Rodríguez-Perea & Servera, 1993), and from the longer water residence time in EP, which, together, may favour particle sedimentation and a larger contribution of allochthonous organic matter to the bottom deposits. In fact, Mazarrasa et al. (2017) observed that allochthonous carbon accounted for more carbon in meadows from EP than in other Balearic meadows, including SM.

At SM shallowest station (SM05, Fig. 4A), pigment assemblages indicated dominance of diatoms (diatoxanthin), seagrasses, and rhodophytes (lutein-zeaxanthin) compared to the deeper stations. A greater abundance of diatoms in the shallowest areas could be related to the diatoms' feature of developing better in turbulent, well-mixed waters (Mabrouk et al., 2011). The greater abundance of seagrass at shallower depths could be explained by higher light availability and, therefore, higher photosynthetic rates and production (Alcoverro et al., 2001). In general, water depth is a key regulator of epiphytes assemblages of seagrasses due to differences in the seagrass and meadow structural characteristics, light penetration, and hydrodynamics (Piazzi et al., 2016 and references therein).

5. Conclusions

The use of fossil pigments is feasible in sheltered vegetative coastal habitats. In this sense, this study pioneers in the use of fossil pigments in *P. oceanica* mats as proxy of phototrophs composition. Fossil pigments can be used in *Posidonia* spp. meadows, where chronologically ordered sequences are highly preserved in the sediments below them (i.e. the mats), but it could be also used in other smaller seagrass located in sheltered areas where sedimentation is not altered.

Our results report changes in phototrophic community composition and production in *P. oceanica* meadows at centennial scales. Analyses suggest that these changes were modulated by both local terrestrial influences and global climate factors. In particular, elevated solar irradiance and air temperature seem to have driven increases in dinoflagellates abundance over the last 150-300 years. Local environmental conditions were most likely responsible for differences in phototrophic communities between basins; apparently due to differences in terrestrial organic matter and nutrient inputs. Depth also influenced the phototrophic community composition, with greater predominance of pigments from diatoms, seagrasses and rodophytes in shallower waters.

These patterns confirm that primary producers in seagrass meadows are under complex hierarchical control by local and global regulatory mechanisms and provide better insights into potential phototrophic responses to global change. Specifically, we infer that global warming may favour the development of autotrophic dinoflagellate assemblages, which could negatively affect the ecosystem functioning by shading and outcompeting the seagrass. Future research could focus on the potential effects of these structural community changes on seagrass ecosystem functioning under predicted climate change scenarios.

Acknowledgements

This research was supported by a PhD scholarship funded by the Spanish Ministry of Science, Innovation and Universities to C. Leiva-Dueñas (FPU15/01934); SUMILEN project (CTM2013-47728-R) funded by the Spanish Ministry of Economy and Competitiveness; and the PALEOPARK project funded by the Spanish Autonomous Organism of National Parks, (ref. 1104/2014). O. Serrano was supported by an ARC DECRA DE170101524. L. López-Merino was supported by a Leverhulme Early Career Fellowship (ECF-2013-530) for the palynological extraction at Brunel University London, and is currently performing the counting and palynological identifications thanks to PALAEOCON, a Marie Skłodowska-Curie Action (H2020-MSCA-IF-2018, Grant agreement ID: 833422) at the Universidade de Santiago de Compostela. Pigment analyses were supported by the Natural Sciences and Engineering Research Council of Canada (NSERC), the Canada Foundation for Innovation (CFI), and the Canada Research Chairs (CRC) programs, the Province of Saskatchewan, University of Regina and Queen’s University Belfast. GDGT analysis was supported by the Netherlands Earth System Science Centre financed by the Dutch Ministry of Education and Science. We thank Deirdre Bateson for pigment analyses, Dr Thomas Hoyle and Manuel Sala for their help in the identification of dinocysts, Karsten Dekker (NIOZ) for GDGT analysis as well as Nerea Piñeiro-Juncal, Anna Thoran and Ambra Milani for their involvement in field work and laboratory analyses. This is a paper of the Group of Benthic Ecology 2014 SGR 120 of the Group of Aquatic Macrophyte Ecology (GAME).

References

Agawin, N.S.R., Ferriol, P., Sintes, E., Moyà, G., 2017. Temporal and spatial variability of in situ nitrogen fixation activities associated with the Mediterranean seagrass *Posidonia oceanica* meadows. Limnol. Oceanogr. 62, 2575–2592. https://doi.org/10.1002/lno.10591

lcover, J , Ballesteros, E , Forn s, J J , Hist ria natural de l’ rxip lag de Cabrera. MOLL-CSIC, Madrid.

Alcoverro, T., Cebrian, E., Ballesteros, E., 2001. The photosynthetic capacity of the seagrass *Posidonia oceanica*: influence of nitrogen and light. J. Exp. Mar. Bio. Ecol. 261, 107–120. https://doi.org/https://doi.org/10.1016/S0022-0981(01)00267-2

Armitage, A.R., Frankovich, T.A., Fourqurean, J.W., 2006. Variable responses within epiphytic and benthic microalgal communities to nutrient enrichment. Hydrobiologia 569, 423–435. https://doi.org/10.1007/s10750-006-0146-8

Armstrong, M., Kudela, R., 2006. Evaluation of California isolates of *Lingulodinium polyedrum* for the production of yessotoxin. African J. Mar. Sci. 28. https://doi.org/10.2989/18142320609504186

Ballesteros, E., Zabala, M., 1993. El bentos: El marc físic., in: Alcover, J.A., Ballesteros, E , Forn s, J J (Eds), Hist ria Natural de l’arxip lag de Cabrera Moll. Monogr. Soc. Hist. Nat. Balears 2, Madrid, pp. 663–685.

Berg, G.M., Balode, M., Purina, I., Purvina, S., Christian, B., Serge, M., 2003. Plankton community composition in relation to availability and uptake of oxidized and reduced nitrogen. Aquat. Microb. Ecol. (Inter-research), 2003 , Vol. 30 , N. 3 , P. 263-274 30. https://doi.org/10.3354/ame030263

Berman, T., 2001. The role of DON and the effect of N:P ratios on occurrence of cyanobacterial blooms: Implications from the outgrowth of *Aphanizomenon* in Lake Kinneret. Limnol. Oceanogr. - LIMNOL Ocean. 46, 443–447. https://doi.org/10.4319/lo.2001.46.2.0443

Blomqvist, P., Pettersson, A., Hyenstrand, P., 1994. Ammonium-Nitrogen - A key regulatory factor causing dominance of non-nitrogen-fixing cyanobacteria in aquatic systems. Arch. Fur Hydrobiol. 132, 141–164.

Borowitzka, M.A., Lavery, P.S., Keulen, M., 2006. Epiphytes of Seagrasses, in: Larkum, A.W.D., Orth, R.J., Duarte, C.M. (Eds.), Seagrasses: Biology, Ecology and Conservation. Springer, Dordrecht, pp. 441–461.

Boudouresque, C.F., Shili, A., Verlaque, M., Paoli, D.C.P., 2009. Regression of Mediterranean seagrasses caused by natural processes and anthropogenic disturbances and stress : a critical review 52, 5–418. https://doi.org/10.1515/BOT.2009.057

Bringué, M., Pospelova, V., Pak, D., 2013. Seasonal production of organic-walled dinoflagellate cysts in an upwelling system: A sediment trap study from the Santa Barbara Basin, California. Mar. Micropaleontol. 100, 34–51. https://doi.org/https://doi.org/10.1016/j.marmicro.2013.03.007

Casazza, G., Mazella, L., 2002. Photosynthetic pigment composition of marine angiosperms: Preliminary characterization of Mediterranean seagrasses. Bull. Mar. Sci. 71, 1171–1181.

Coleman, V.L., Burkholder, J.M., 1994. Community structure and productivity of epiphytic microalgae on eelgrass (*Zostera marina* L.) under water-column nitrate enrichment. J. Exp. Mar. Bio. Ecol. 179, 29–48. https://doi.org/https://doi.org/10.1016/0022-0981(94)90015-9

Craine, J. M., Brookshire, E. N. J., Cramer, M. D., Hasselquist, N. J., Koba, K., Mar. E., Wang, L., 2015. Ecological interpretations of nitrogen isotope ratios of terrestrial plants and soils. Plant Soil, 396(1), 1–26. https://doi.org/10.1007/s11104-015-2542-1

de los Santos, C.B., Krause-Jensen, D., Alcoverro, T., Marbà, N., Duarte, C.M., van Katwijk, M.M., Pérez, M., Romero, J., Sánchez-Lizaso, J.L., Roca, G., Jankowska, E., Pérez-Lloréns, J.L., Fournier, J., Montefalcone, M., Pergent, G., Ruiz, J.M., Cabaço, S., Cook, K., Wilkes, R.J., Moy, F.E., Trayter, G.M.-R., Arañó, X.S., de Jong, D.J., Fernández-Torquemada, Y., Auby, I., Vergara, J.J., Santos, R., 2019. Recent trend reversal for declining European seagrass meadows. Nat. Commun. 10, 3356. https://doi.org/10.1038/s41467-019-11340-4

Delgado, O., Ruiz, J., Pérez, M., Romero, J., Ballesteros, E., 1999. Effects of fish farming on seagrass (*Posidonia oceanica*) in a Mediterranean bay: seagrass decline after organic loading cessation. Oceanol. Acta 22, 109–117. https://doi.org/https://doi.org/10.1016/S0399-1784(99)80037-1

Donald, D., Bogard, M., Finlay, K., Leavitt, P., 2011. Comparative effects of urea, ammonium, and nitrate on phytoplankton abundance, community composition, and toxicity in hypereutrophic freshwaters. Limnol. Oceanogr. 56, 2161. https://doi.org/10.4319/lo.2011.56.6.2161

Egozcue, J.J., Pawlowsky-Glahn, V., Mateu-Figueras, G., Barceló-Vidal, C., 2003. Isometric logratio transformations for compositional data analysis. Math. Geol. 35, 279–300. https://doi.org/https://doi.org/10.1023/A:1023818214614

Fægri, K., Iversen, J., 1989. Textbook of Pollen Analysis, in: Fægri, K., Kaland, P.E., Krzywinski, K. (Eds), 4th ed. John Wiley and Sons, Chichester (UK). 328 pp.

Filzmoser, P., Hron, K., Reimann, C., 2010. The bivariate statistical analysis of environmental (compositional) data. Sci. Total Environ. 408, 4230–4238. https://doi.org/https://doi.org/10.1016/j.scitotenv.2010.05.011

Frankovich, T., Gaiser, E., Zieman, J., Wachnicka, A., 2006. Spatial and temporal distributions of epiphytic diatoms growing on *Thalassia testudinum* Banks ex König: Relationships to water quality. Hydrobiologia 569, 259–271. https://doi.org/10.1007/s10750-006-0136-x

Fu, F.X., Tatters, A.O., Hutchins, D.A., 2012. Global change and the future of harmful algal blooms in the ocean. Mar. Ecol. Prog. Ser. 470, 207–233.

Glibert, P., Heil, C., Hollander, D., Revilla, M., Hoare, A., Alexander, J., Murasko, S., 2004. Evidence for dissolved organic nitrogen and phosphorus uptake during a cyanobacterial bloom in Florida Bay. Mar. Ecol. Prog. Ser. 280, 73–83. https://doi.org/10.3354/meps280073

Glibert, P., Wilkerson, F., Dugdale, R., Parker, A., Alexander, J., Blaser, S., Murasko, S., 2014. Phytoplankton communities from San Francisco Bay Delta respond differently to oxidized and reduced nitrogen substrates- even under conditions that would otherwise suggest nitrogen sufficiency. Front. Mar. Sci. 1, 1–16. https://doi.org/10.3389/fmars.2014.00017

Hannach, G., Sigleo, A., 1998. Photoinduction of UV-absorbing compounds in six species of marine phytoplankton. Mar. Ecol. Prog. Ser. 174, 207–222. https://doi.org/10.3354/meps174207

Hauxwell, J., Cebrián, J., Furlong, C., Valiela, I., 2001. Macroalgal canopies contribute to eelgrass (*Zostera marina*) decline in temperate estuarine ecosystems. Ecology 82, 1007–1022. https://doi.org/10.2307/2679899

Hay, W.W., 1974. Introduction, in: Hay, W.W. (Ed.), Studies in Paleo-Oceanography. SEPM Society for Sedimentary Geology. https://doi.org/https://doi.org/10.2110/pec.74.20

Heil, C., Revilla, M., Glibert, P., Murasko, S., 2007. Nutrient quality drives phytoplankton community composition on the West Florida Shelf. Limnol. Oceanogr. 52, 1067–1078. https://doi.org/10.4319/lo.2007.52.3.1067

Hemminga, M.A., Duarte, C.M., 2000. Seagrass Ecology. Cambridge University Press. https://doi.org/10.1017/CBO9780511525551

Holmer, M., Duarte, C.M., Marbá, N., 2003. Sulfur cycling and seagrass (*Posidonia oceanica)* status in carbonate sediments. Biogeochemistry 66, 223–239. https://doi.org/10.1023/B:BIOG.0000005326.35071.51

Holmer, M., Duarte, C., Boschker, H., Barrón, C., 2004. Carbon cycling and bacterial carbon sources in pristine and impacted Mediterranean seagrass sediments. Aquat. Microb. Ecol. 36, 227–237. https://doi.org/10.3354/ame036227

Holmer, M., Duarte, C.M., Marbá, N., 2005. Iron additions reduce sulfate reduction rates and improve seagrass growth on organic-enriched carbonate sediments. Ecosystems 8, 721–730. https://doi.org/10.1007/s10021-003-0180-6

Hopmans, E., Weijers, J., Schefuß, E., Herfort, L., Sinninghe-Damste, J., Schouten, S., 2004. A novel proxy for terrestrial organic matter in sediments based on branched and isoprenoid tetraether lipids. Earth Planet. Sci. Lett. 224, 107–116. https://doi.org/10.1016/j.epsl.2004.05.012

Hurrell, J , 200 N O Index Data provided by the Climate nalysis Section: —N O Station Based (nnual)‖ [WWW Document] Updat Regul URL https://climatedataguide.ucar.edu/climate-data/hurrell-north-atlantic-oscillation-nao-index-station-based (accessed 7.13.19).

Johnson, M.P., Edwards, M., Bunker, F., Maggs, C.A., 2005. Algal epiphytes of *Zostera marina*: Variation in assemblage structure from individual leaves to regional scale. Aquat. Bot. 82, 12–26. https://doi.org/https://doi.org/10.1016/j.aquabot.2005.02.003

Kaal, J., Serrano, O., Nierop, K.G.J., Schellekens, J., Martínez-Cortizas, A., Mateo, M. A., 2016. Molecular composition of plant parts and sediment organic matter in a Mediterranean seagrass (*Posidonia oceanica*) mat. Aquat. Bot. 133, 50–61. https://doi.org/10.1016/j.aquabot.2016.05.009

Kobashi, T., Goto-Azuma, K., Box, J., Gao, C., Nakaegawa, T., 2013. Causes of Greenland temperature variability over the past 4000 yr: Implications for northern hemispheric temperature changes. Clim. Past 9, 2299–2317. https://doi.org/10.5194/cp-9-2299-2013

Koch, E.W., 2001. Beyond light: Physical, geological, and geochemical parameters as possible submersed aquatic vegetation habitat requirements. Estuaries 24, 1–17. https://doi.org/10.2307/1352808

Kowalewska, G., Wawrzyniak-Wydrowska, B., Szymczak-Żyła, M , 2004 Chlorophyll *a* and its derivatives in sediments of the Odra estuary as a measure of its eutrophication. Mar. Pollut. Bull. 49, 148–153. https://doi.org/https://doi.org/10.1016/j.marpolbul.2004.02.003

Lavaud, J., Rousseau, B., van Gorkom, H., Etienne, A.-L., 2002. Influence of the diadinoxanthin pool size on photoprotection in the marine planktonic diatom *Phaeodactylum tricornutum*. Plant Physiol. 129, 1398–1406. https://doi.org/10.1104/pp.002014

Lavery, P.S., Reid, T., Hyndes, G.A., 2007. Effect of leaf movement on epiphytic algal biomass of seagrass leaves . Mar. Ecol. Prog. Ser. 338, 97–106.

Laviale, M., Jacques, N., 2011. Relationships between pigment ratios and growth irradiance in 11 marine phytoplankton species. Mar. Ecol. Prog. Ser. 425, 63–77. https://doi.org/10.3354/meps09013

Leavitt, P., Hodgson, D., 2001. Sedimentary pigments, in: Smol, J.P., Birks, H.J.B., Last, W.M. (Eds.), Tracking Environmental Changes Using Lake Sediments. Volume 3: Terrestrial, Algal, and Siliceous Indicators. Kluwer Academic Publishers, Dordrecht, The Netherlands, pp. 295–325

Leiva-Dueñas, C., López-Merino, L., Serrano, O., Martínez Cortizas, A., Mateo, M.A., 2018. Millennial-scale trends and controls in *Posidonia oceanica* (L. Delile) ecosystem productivity. Glob. Planet. Change 169. https://doi.org/10.1016/j.gloplacha.2018.07.011

Leri, A.C., Mayer, L.M., Thornton, K.R., Northrup, P.A., Dunigan, M.R., Ness, K.J., Gellis, A.B., 2015. A marine sink for chlorine in natural organic matter. Nature Geosci. 8, 620–624. https://doi.org/10.1038/ngeo2481

Leroy, S.A.G., Lahijani, H.A.K., Reyss, J.-L., Chalié, F., Haghani, S., Shah-Hosseini, M., Shahkarami, S., Tudryn, A., Arpe, K., Habibi, P., Nasrollahzadeh, H.S., Makhlough, A., 2013. A two-step expansion of the dinocyst *Lingulodinium machaerophorum* in the Caspian Sea: The role of changing environment. Quat. Sci. Rev. 77, 31–45. https://doi.org/https://doi.org/10.1016/j.quascirev.2013.06.026

Lewis, J., Hallett, R., 1997. *Lingulodinium polyedrum* (*Gonyaulax polyedra*) a blooming dinoflagellate. Oceanogr. Mar. Biol. 35, 97–161.

Lindell, D., Post, A.F., 2001. Ecological aspects of ntcA gene expression and its use as an indicator of the nitrogen status of marine *Synechococcus* spp. Appl. Environ. Microbiol. 67, 3340–3349. https://doi.org/10.1128/AEM.67.8.3340-3349.2001

Lo Iacono, C., Mateo, M.A., Gràcia, E., Guasch, L., Carbonell, R., Serrano, L., Serrano, O., Dañobeitia, J., 2008. Very high-resolution seismo-acoustic imaging of seagrass meadows (Mediterranean Sea): Implications for carbon sink estimates. Geophys. Res. Lett. 35, L18601. https://doi.org/10.1029/2008GL034773

López-Merino, L., Serrano, O., Adame, M.F., Mateo, M.Á., Martínez Cortizas, A., 2015. Glomalin accumulated in seagrass sediments reveals past alterations in soil quality due to land-use change. Glob. Planet. Change 133, 87–95. https://doi.org/10.1016/j.gloplacha.2015.08.004

López-Merino, L., Colás-Ruiz, N.R., Adame, M.F., Serrano, O., Martínez Cortizas, A., Mateo, M.A., 2017. A six thousand-year record of climate and land-use change from Mediterranean seagrass mats. J. Ecol. 105, 1267–1278. https://doi.org/10.1111/1365-2745.12741

López-Sáez, J. a., López-Merino, L., Mateo, M.A., Serrano, Ó., Pérez-Díaz, S., Serrano, L., 2009. Palaeoecological potential of the marine organic deposits of *Posidonia oceanica*: A case study in the NE Iberian Peninsula. Palaeogeogr. Palaeoclimatol. Palaeoecol. 271, 215–224. https://doi.org/10.1016/j.palaeo.2008.10.020

Mabrouk, L., Hamza, A., Brahim, M. Ben, Bradai, M.-N., 2011. Temporal and depth distribution of microepiphytes on *Posidonia oceanica* (L.) Delile leaves in a meadow off Tunisia. Mar. Ecol. 32, 148–161. https://doi.org/10.1111/j.1439-0485.2011.00432.x

Mabrouk, L., Hamza, A., Mahfoudi, M., Bradai, M., 2012. Spatial and temporal variations of epiphytic *Ostreopsis siamensis* on *Posidonia oceanica* (L.) Delile leaves in Mahdia (Tunisia). Cah. Biol. Mar. 53, 419–427.

Mabrouk, L., Brahim, M. Ben, Hamza, A., Bradai, M., 2014. Temporal and spatial zonation of macroepiphytes on *Posidonia oceanica* (L.) Delile leaves in a meadow off. Mar. Ecol. 36, 77–92. https://doi.org/10.1111/maec.12118

Marbà, N., Duarte, C.M., Holmer, M., Martínez, R., Basterretxea, G., Orfila, A., Jordi, A., Tintoré, J., 2002. Effectiveness of protection of seagrass (*Posidonia oceanica*) populations in Cabrera National Park (Spain). Environ. Conserv. 29, 509–518. https://doi.org/DOI: 10.1017/S037689290200036X

Marbà, N., Duarte, C.M., Holmer, M., Calleja, M.L., Álvarez, E., Díaz-Almela, E., Garcias-Bonet, N., 2008. Sedimentary iron inputs stimulate seagrass (*Posidonia oceanica*) population growth in carbonate sediments. Estuar. Coast. Shelf Sci. 76, 710–713. https://doi.org/https://doi.org/10.1016/j.ecss.2007.07.021

Marbà, N., Duarte, C., 2010. Mediterranean warming triggers seagrass (*Posidonia oceanica*) shoot mortality. Glob. Chang. Biol. 16, 2366–2375. https://doi.org/10.1111/j.1365-2486.2009.02130.x

Mateo, M.A., Romero, J., Pérez, M., Littler, M.M., Littler, D.S., 1997. Dynamics of millenary organic deposits resulting from the growth of the mediterranean seagrass *Posidonia oceanica*. Estuar. Coast. Shelf Sci.44, 103–110.

Mateo, M.A., Cebrián, J., Dunton, K., Mutchler, T., 2006. Carbon flux in seagrass ecosystems. Biol. Ecol. Conserv. 159–192.

Mateo, M.A., Renom, P., Michener, R.H., 2010. Long-term stability in the production of a NW Mediterranean *Posidonia oceanica* (L.) Delile meadow. Palaeogeogr. Palaeoclimatol. Palaeoecol. 291, 286–296. https://doi.org/10.1016/j.palaeo.2010.03.001

Mazarrasa, I., Marba, N., Garcia-Orellana, J., Masqué, P., Arias-Ortiz, A., Duarte, C., 2017. Dynamics of carbon sources supporting burial in seagrass sediments under increasing anthropogenic pressure. Limnol. Oceanogr. 62, 1451–1465. https://doi.org/10.1002/lno.10509

McGlathery, K., Sundbäck, K., Anderson, I., 2007. Eutrophication in shallow coastal bays and lagoons: The role of plants in the coastal filter. Mar. Ecol. Prog. Ser. 348, 1–18.

Moncer, M., Hamza, A., Feki, W., Mabrouk, L., Hassen, M., 2017. Variability patterns of epibenthic microalgae in eastern Tunisian coasts. Sci. Mar. 81, 487–498. https://doi.org/10.3989/scimar.04651.17A

Moore, K.A., Wetzel, R.L., 2000. Seasonal variations in eelgrass (*Zostera marina* L.) responses to nutrient enrichment and reduced light availability in experimental ecosystems. J. Exp. Mar. Bio. Ecol. 244, 1–28. https://doi.org/10.1016/S0022-0981(99)00135-5

Morton, R.A., White, W.A., 1997. Characteristics of and corrections for core shortening in unconsolidated sediments. J. Coast. Res. 13, 761–769.

Nesti, U., Piazzi, L., Balata, D., 2009. Variability in the structure of epiphytic assemblages of the Mediterranean seagrass *Posidonia oceanica* in relation to depth. Mar. Ecol. 30, 276–287. https://doi.org/10.1111/j.1439-0485.2008.00275.x

Olsen, J., Anderson, N.J., Knudsen, M.F., 2012. Variability of the North Atlantic Oscillation over the past 5,200 years. Nature Geosci. 5, 808–812. https://doi.org/10.1038/ngeo1589

Orfila, A., Jordi, A., Basterretxea, G., Vizoso, G., Marba, N., Duarte, C., Werner, F.E., Tintoré, J., 2005. Residence time and *Posidonia oceanica* in Cabrera Archipelago National Park, Spain. Cont. Shelf Res. 25, 1339–1352. https://doi.org/10.1016/j.csr.2005.01.004

Orfila, M., Hernández, M., Cau Ontiveros, M., 1992. Nuevos datos sobre el poblamiento antiguo de la isla de Cabrera (Baleares): Una posible factoría de salazones. Sagvntum 25. https://doi.org/10.7203/SAGVNTVM..3644

Paerl, H., Huisman, J., 2008. Blooms Like It Hot. Science 320, 57–58. https://doi.org/10.1126/science.1155398

Paz, B., Riobó, P., Fernández, M.L., Fraga, S., Franco, J.M., 2004. Production and release of yessotoxins by the dinoflagellates *Protoceratium reticulatum* and *Lingulodinium polyedrum* in culture. Toxicon 44, 251–258. https://doi.org/https://doi.org/10.1016/j.toxicon.2004.05.021

Penna, A., Bertozzini, E., Battocchi, C., Galluzzi, L., Giacobbe, M.G., Vila, M., Garces, E., Lugliè, A., Magnani, M., 2006. Monitoring of HAB species in the Mediterranean Sea through molecular methods. J. Plankton Res. 29, 19–38. https://doi.org/10.1093/plankt/fbl053

Pérez, M., Invers, O., Ruiz Fernández, J.M., Frederiksen, M., Holmer, M., 2007. Physiological responses of the seagrass *Posidonia oceanica* to elevated organic matter content in sediments: An experimental assessment. J. Exp. Mar. Bio. Ecol. 344, 149–160. https://doi.org/10.1016/j.jembe.2006.12.020

Piazzi, L., Balata, D., Ceccherelli, G., 2016. Epiphyte assemblages of the Mediterranean seagrass *Posidonia oceanica*: An overview. Mar. Ecol. 37, 3–41. https://doi.org/10.1111/maec.12331

Piñeiro Juncal, N., Mateo, M.Á., Holmer, M., Martínez-Cortizas, A., 2018. Potential microbial functional activity along a *Posidonia oceanica* soil profile. Aquat. Microb. Ecol. 81. https://doi.org/10.3354/ame01872

Pospelova, V., Pedersen, T., Anne, de V., 2006. Dinoflagellate cysts as indicators of climatic and oceanographic changes during the past 40 kyr in the Santa Barbara Basin, Southern California. Paleoceanography 21. https://doi.org/10.1029/2005PA001251

Prado, P., Alcoverro, T., Martínez-Crego, B., Vergés, A., Pérez, M., Romero, J., 2007. Macrograzers strongly influence patterns of epiphytic assemblages in seagrass meadows. J. Exp. Mar. Bio. Ecol. 350, 130–143. https://doi.org/https://doi.org/10.1016/j.jembe.2007.05.033

R Core Team, 2018. R: A Language and Environment for Statistical Computing.

Rabalais, N.N., Atilla, N., Normandeau, C., Turner, R.E., 2004. Ecosystem history of Mississippi River-influenced continental shelf revealed through preserved phytoplankton pigments. Mar. Pollut. Bull. 49, 537–547. https://doi.org/https://doi.org/10.1016/j.marpolbul.2004.03.017

Ralph, P., Tomasko, D., Moore, K., Seddon, S., Macinnis-Ng, C., 2006. Human Impacts on Seagrasses: Eutrophication, Sedimentation and Contamination, in: Larkum, A.W.D., Orth, R.J., Duarte, C.M. (Eds.), Seagrasses: Biology, Ecology and Conservation. Springer, Dordrecht, pp. 567–593.

Reuss, N., Conley, D.J., Bianchi, T.S., 2005. Preservation conditions and the use of sediment pigments as a tool for recent ecological reconstruction in four Northern European estuaries. Mar. Chem. 95, 283–302. https://doi.org/https://doi.org/10.1016/j.marchem.2004.10.002

Reuss, N., Leavitt, P.R., Hall, R.I., Bigler, C., Hammarlund, D., 2010. Development and application of sedimentary pigments for assessing effects of climatic and environmental changes on subarctic lakes in northern Sweden. J. Paleolimnol. 43, 149–169. https://doi.org/10.1007/s10933-009-9323-x

Riera, T., Blasco, D., 1967. Surface plankton of the Balear sea in July 1966. Investig. Pesq. 31, 463–484.

Roberts, N., Moreno, A., Valero-Garcés, B.L., Corella, J.P., Jones, M., Allcock, S., Woodbridge, J , Morell n, M , Luterbacher, J , Xoplaki, E , Türkeş, M , 20 2 Palaeolimnological evidence for an east–west climate see-saw in the Mediterranean since AD 900. Glob. Planet. Change 84–85, 23–34. https://doi.org/https://doi.org/10.1016/j.gloplacha.2011.11.002

Rodríguez-Perea, A., Servera, J., 1993. Geomorfologia, in: Alcover, J., Ballesteros, E., Forn s, J (Eds), Hist ria Natural de l’arxip lag de Cabrera Moll. Monogr. Soc. Hist. Nat. Balears 2, Madrid, pp. 33–60.

Rose, N.L., Yang, H., Turner, S.D., Simpson, G.L., 2012. An assessment of the mechanisms for the transfer of lead and mercury from atmospherically contaminated organic soils to lake sediments with particular reference to Scotland, UK. Geochim. Cosmochim. Acta 82, 113–135. https://doi.org/https://doi.org/10.1016/j.gca.2010.12.026

Savva, I., Bennett, S., Roca, G., Jordà, G., Marba, N., 2018. Thermal tolerance of Mediterranean marine macrophytes: Vulnerability to global warming. Ecol. Evol. 8. https://doi.org/10.1002/ece3.4663

Schouten, S., Huguet, C., Hopmans, E.C., Kienhuis, M.V.M., Sinninghe Damsté, J.S., 2007. Analytical methodology for TEX86 paleothermometry by high-performance liquid chromatography/atmospheric pressure chemical ionization-mass spectrometry. Anal. Chem. 79, 2940–2944. https://doi.org/10.1021/ac062339v

Sellner, K.G., Doucette, G.J., Kirkpatrick, G.J., 2003. Harmful algal blooms: causes, impacts and detection. J. Ind. Microbiol. Biotechnol. 30, 383–406. https://doi.org/10.1007/s10295-003-0074-9

Serrano, O., Mateo, M. A, Dueñas-Bohórquez, A, Renom, P., López-Sáez, J. A, Martínez Cortizas, A, 2011. The *Posidonia oceanica* marine sedimentary record: A Holocene archive of heavy metal pollution. Sci. Total Environ. 409, 4831–40. https://doi.org/10.1016/j.scitotenv.2011.08.001

Serrano, O., Mateo, M. A., Renom, P., Julià, R., 2012. Characterization of soils beneath a *Posidonia oceanica* meadow. Geoderma 185, 26–36. https://doi.org/10.1016/j.geoderma.2012.03.020

Serrano, O., Martínez-Cortizas, A., Mateo, M.A., Biester, H., Bindler, R., 2013. Millennial scale impact on the marine biogeochemical cycle of mercury from early mining on the Iberian Peninsula. Global Biogeochem. Cycles 27, 21–30. https://doi.org/10.1029/2012GB004296

Serrano, O., Lavery, P.S., Rozaimi, M., Mateo, M.A., 2014. Influence of water depth on the carbon sequestration capacity of seagrasses. Global Biogeochem. Cycles 28, 950–961. https://doi.org/10.1002/2014GB00487

Serrano, O., Lavery, P.S., López-Merino, L., Ballesteros, E., Mateo, M.A., 2016a. Location and associated carbon storage of erosional escarpments of seagrass *Posidonia* Mats. Front. Mar. Sci. 3, 42. https://doi.org/10.3389/fmars.2016.00042

Serrano, O., Davis, G., Lavery, P.S., Duarte, C.M., Martinez-cortizas, A., Angel, M., Masqué, P., Arias-Ortiz, A., Rozaimi, M., Kendrick, G.A., 2016b. Reconstruction of centennial-scale fluxes of chemical elements in the Australian coastal environment using seagrass archives. Sci. Total Environ. 541, 883–894. https://doi.org/10.1016/j.scitotenv.2015.09.017

Serrano, O., Lavery, P., Masque, P., Inostroza, K., Bongiovanni, J., Duarte, C., 2016c. Seagrass sediments reveal the long-term deterioration of an estuarine ecosystem. Glob. Chang. Biol. 22, 1523–1531. https://doi.org/10.1111/gcb.13195

Short, F.T., Wyllie-Echeverria, S., 1996. Natural and human-induced disturbance of seagrasses. Environ. Conserv. 23, 17–27. https://doi.org/10.1017/S0376892900038212

Simpson, G.L., 2018. Modelling palaeoecological time series using generalised additive models. Front. Ecol. Evol. 6, 149. https://doi.org/10.3389/fevo.2018.00149

Sobrino, C., Garcia-Gil, S., Iglesias, J., Carreño, N., da Costa, J., Díaz Varela, R., Judd, A., 2012. Environmental change in the Ría de Vigo, NW Iberia, since the mid-Holocene: New palaeoecological and seismic evidence. Boreas 41, 578–601.

https://doi.org/10.1111/j.1502-3885.2012.00255.x

Spalding, M., Taylor, M., Ravilious, C., Short, F., Green, E., 2003. Global overview: The distribution and status of seagrasses, in: Green, E.P., Short, F.T. (Eds.), World Atlas of Seagrasses: Present Status and Future Conservation. University of California Press, Berkeley, pp. 5–26.

Spilling, K., Kremp, A., Klais, R., Olli, K., Tamminen, T., 2014. Spring bloom community change modifies carbon pathways and C : N : P : Chla stoichiometry of coastal material fluxes. Biogeosciences 11, 7275–7289. https://doi.org/10.5194/bg-11-7275-2014

Spilling, K., Olli, K., Lehtoranta, J., Kremp, A., Tedesco, L., Tamelander, T., Klais, R., Peltonen, H., Tamminen, T., 2018. Shifting Diatom—Dinoflagellate Dominance During Spring Bloom in the Baltic Sea and its Potential Effects on Biogeochemical Cycling. Front. Mar. Sci. 5, 327. https://doi.org/10.3389/fmars.2018.00327

Templ, M., Hron, K., Filzmoser, P., 2011. robCompositions: an R-package for robust statistical analysis of compositional data, in: Pawlowsky-Glahn, V., Buccianti, A. (Eds.), Compositional Data Analysis: Theory and Applications. John Wiley and Sons, Chichester (UK), pp. 341–355.

Trouet, V., Esper, J., Graham, N., Baker, A., Scourse, J., Frank, D., 2009. Persistent Positive North Atlantic Oscillation Mode Dominated the Medieval Climate Anomaly. Science 324, 78–80. https://doi.org/10.1126/science.116634

Tsirika, A., Skoufas, G., Haritonidis, S., 2007. Seasonal and bathymetric variations of epiphytic macroflora on *Posidonia oceanica* (L.) Delile leaves in the National Marine Park of Zakynthos (Greece). Mar. Ecol. 28, 146–153. https://doi.org/10.1111/j.1439-0485.2007.00170.x

Turki, S., 2005. Distribution of toxic dinoflagellates along the leaves of seagrass Posidonia oceanica and Cymodocea nodosa from the Gulf of Tunis. Cah. Biol. Mar. 46, 29–34.

Versteegh, G., Blokker, P., 2004. Resistant macromolecules of extant and fossil microalgae. Phycol. Res. 52, 325–339. https://doi.org/10.1111/j.1440-183.2004.00361.x

Viaroli, P., Bartoli, M., Giordani, G., Naldi, M., Orfanidis, S., Zaldivar, J.M., 2008. Community shifts, alternative stable states, biogeochemical controls and feedbacks in eutrophic coastal lagoons: a brief overview. Aquat. Conserv. Mar. Freshw. Ecosyst. 18, S105–S117. https://doi.org/10.1002/aqc.956

Vieira, L., Solanki, S., Krivova, N., Usoskin, I., 2011. Evolution of the solar irradiance during the Holocene. Astron. Astrophys. 531. https://doi.org/10.1051/0004-6361/201015843

Vives, F , spectes Hidrogràfics i Planct nics dels Voltants de l’ rxip lag de Cabrera, in: Alcover, J.A., Ballesteros, E., Fornós, J.J. (Eds.), Història Natural de l’arxipèlag de Cabrera. Moll. Monogr. Soc. Hist. Nat. Balears 2, Madrid, pp. 487–502.

Wasmund, N., Kownacka, J., Göbel, J., Jaanus, A., Johansen, M., Jurgensone, I., Lehtinen, S., Powilleit, M., 2017. The Diatom/Dinoflagellate Index as an Indicator of Ecosystem Changes in the Baltic Sea 1. Principle and Handling Instruction. Front. Mar. Sci. 4. https://doi.org/10.3389/fmars.2017.00022

Wells, M.L., Trainer, V.L., Smayda, T.J., Karlson, B.S.O., Trick, C.G., Kudela, R.M., Ishikawa, A., Bernard, S., Wulff, A., Anderson, D.M., Cochlan, W.P., 2015. Harmful algal blooms and climate change: Learning from the past and present to forecast the future. Harmful Algae 49, 68–93.

https://doi.org/https://doi.org/10.1016/j.hal.2015.07.009

Wood, S.N., 2003. Thin plate regression splines. J. R. Stat. Soc. Ser. B 65, 95–114.

Wood, S.N., 2004. Stable and efficient multiple smoothing parameter estimation for generalized additive models. J. Am. Stat. Assoc. 99, 673–686.

Wood, S.N., N., Pya, Säfken, B., 2016. Smoothing parameter and model selection for general smooth models (with discussion). J. Am. Stat. Assoc. 111, 1548–1575.

Wood, S.N., 2017. Generalized Additive Models: An Introduction with R, 2nd ed. Chapman and Hall/CRC.

Figures

Figure 1. Schematic diagram illustrating how nutrient and sediment inputs affect aquatic primary producers in seagrass meadows. Zooms are for micro-epiphytic community composition. Diagram made using image vectors from Image library in Integration and Application Network (ian.umces.edu).

Figure 2. Location of the Cabrera Archipelago as well as *P. oceanica* and *Cymodocea* meadows areal coverage in two bays: Santa Maria (SM) and Es Port (EP). Red dots indicate the core locations. The number stands for the sampling water depth (in meters below sea level).

Figure 3. A) Bayesian age depth-models of Cabrera Island cores using Bacon.R software (Blaauw & Christen, 2011). Lead-210 (in green) and radiocarbon (in blue) dates were included in the age-depth models. Radiocarbon dates were calibrated using the *marine 13* calibration curve (Reimer et al., 2013) and corrected for a local marine reservoir effect (mean ± SD; $\Delta R = 26 \pm 24$ years; Riera Rullan, 2016) The red dashed curve shows the —best‖ model based on the weighted mean age for each depth. Individual radiocarbon dates are shown in probability density functions of calibrated ages. The grey area indicates the uncertainty envelope of the model with grey dashed curves indicating 95% confidence intervals. The vertical, dashed black line on the EP05 model denotes a hiatus. B) Notched box-plot of accumulation rates for each of the sampled cores.

Figure 4. $PCA_{pigments}$ run to explore potential associations in the community of primary producers as recorded by fossil pigment concentrations in the cores. **A)** Clr-biplot of sample scores. Red ellipse indicates samples from EP and blue ellipse indicates samples from SM. **B)** Depth records of the $PC_{pigments}$ scores. Black solid lines indicate fitted smooth functions of time (GAM models, formula = y ~ s(x)) and grey shaded regions are 95% point-wise confidence intervals. Only GAMs with significant trends are shown ($p>0.05$). Algal groups associated to pigments are in Table 3.

Figure 5. $PCA_{environmental}$ run to decipher relationships between fossil pigment composition and explicative variables: BIT index -an index of the relative abundance of terrestrial organic matter versus marine input in marine sediments (Hopmans et al., 2004), Total Solar Irradiance (TSI, Vieira et al., 2011), Index of North Atlantic Oscillation (NAO, Hurrell, 2003; Trouet et al., 2009; Olsen et al., 2012), Northern-Hemisphere Temperature (NHT, Kobashi et al., 2013), grain-size distribution, content of organic matter (OM), XRF-measured elements (Fe, Si, Ti, K, Ca, S, Cl and Br), carbon and nitrogen stable isotopes, chl-*a* and β-carotenes, and a pigment preservation index (chl-*a*/pheophytin *a*). **A)** Clr-biplot of sample scores. **B)** Depth records of the $PC_{environmental}$ scores. Black solid lines indicate fitted smooth functions of time (GAM models, formula = y ~ s(x)) and grey shaded regions are 95% point-wise confidence intervals. Only GAMs with significant trends are shown ($p>0.05$). Algal groups associated to pigments are in Table 3.

Figure 6. Dinocyst concentrations records of cores EP05 and SM25 plotted together with $PC1_{pigments}$ scores. Positive scores of $PC1_{pigments}$ are related with higher concentrations of diadinoxanthin. Coloured solid lines indicate fitted smooth functions of time (GAM models, formula = y ~ s(x)) and grey shaded regions are 95% point-wise confidence intervals. Only GAMs with significant trends are shown ($p > 0.05$).

Figure 7. Differences between fitted trends in the scores of $PC1_{pigments}$ and dinocysts records for the last 250 years in EP05. Black solid lines indicate differences between fitted smooth functions of time (GAM models, formula = y ~ s(x)) of $PC1_{pigments}$ scores, concentrations of total dinocysts (TC), *Lingulodinium machaerophorum* (LM) and *Spiniferites* spp. (SS). Grey shaded regions are 95% point-wise confidence intervals on these differences.

Tables

Table 1. Details of the five cores taken from *Posidonia oceanica* meadows at two bays in the Cabrera Island (Balearic Islands, Spain).

Core ID	**Coordinates**		**Sampling location**	**Water depth** (m)	**Compressed length** (cm)	**Decompressed length** (cm)	**Compression** (%)
SM05	39º9'0"N	2º56'57"E	Santa María Bay	5	49	83	42.4
SM10	39º9'3"N	2º56'55"E	Santa María Bay	10	134	161	18.3
SM15	39º9'6"N	2º56'53"E	Santa María Bay	15	113	138	19.3
SM25	39º9'12"N	2º56'44"E	Santa María Bay	25	84	89	5.6
EP05	39º8'42"N	2º55'60"E	Es Port Bay	~ 5	88	98	17

Table 2. Radiocarbon dates in the *P. oceanica* mat cores retrieved at the Cabrera Island. The *marine 13* ^{14}C calibration curve (Reimer et al., 2013) was used for calibration of the radiocarbon dates together with and a local marine reservoir effect (mean ± SD; ΔR = 26 ± 24 years; Riera Rullan, 2016).

Core	Laboratory code	Decompressed depth (cm)	AMS ^{14}C date (yr BP)						Weighted mean age
EP05	D-AMS 014002	32	398	±	23	58.5	–	92.4	75.8
	D-AMS 019447	34	379	±	24	66.7	–	108	87.1
	D-AMS 014003	43	467	±	27	104	–	190	141.3
	D-AMS 012768	54	502	±	27	166	–	277	215.4
	D-AMS 029626	60	545	±	30	202	–	349	263.6
	D-AMS 019448	64	1741	±	28	1185	–	1531	1369
	D-AMS 012769	75	1940	±	26	1305	–	1620	1468.9
	D-AMS 012770	96	1788	±	29	1473	–	1473	1651.6
SM05	D-AMS 012771	57	75	±	26	18.8	–	51.1	33.9
	D-AMS 012772	68	105	±	28	43.2	–	87.4	64.6
	D-AMS 013117	78	366	±	25	66.5	–	120	92.9
	D-AMS 012773	79	439	±	25	69.1	–	122	95.7
SM10	D-AMS 019434	34	104	±	25	-0.9	–	7.2	3.2
	D-AMS 019436	58	449	±	28	83.9	–	163	117.6
	D-AMS 019437	63	384	±	29	103	–	138	141.1
	D-AMS 019438	70	479	±	26	130	–	228	177.1
	D-AMS 022098	88	593	±	61	225	–	334	275.2
	D-AMS 022099	110	740	±	34	348	–	462	405.6
	D-AMS 022100	124	970	±	45	434	–	551	494.6
	D-AMS 022102	152	1063	±	43	588	–	740	657.5
SM15	D-AMS 019444	50	610	±	24	89.4	–	242	151.8
	D-AMS 012774	55	573	±	23	126	–	305	207.6
	UBA-32342	75	1732	±	32	752	–	1154	996.7
	D-AMS 019445	78	1508	±	29	899	–	1169	1044.9
	D-AMS 012775	89	1583	±	23	1058	–	1269	1163.3
	D-AMS 012776	104	2447	±	32	1269	–	1703	1477.9
	D-AMS 029627	120	2106	±	29	1482	–	1845	1664.7
	D-AMS 029628	135	1556	±	29	1634	–	2098	1830.1

	D-AMS 019439	8	216	±	46	-49.5	–	63.9	7.3
	D-AMS 014000	28	508	±	20	76.7	–	243	165.3
	D-AMS 019440	35	608	±	27	144	–	303	229.2
	D-AMS 014001	39	604	±	29	181	–	383	271.8
SM25	D-AMS 012777	49	1000	±	27	427	–	637	537.7
	D-AMS 019441	56	1234	±	27	628	–	852	728
	D-AMS 012778	70	1957	±	24	1170	–	1525	1374.6
	D-AMS 019442	76	1985	±	25	1428	–	1533	1532.2
	D-AMS 012779	89	2178	±	28	1619	–	1871	1748.5

Table 3. Pigments identified in the *P. oceanica* mat cores in this study as well as their taxonomic affinities.

Pigment	Algal group(s)
Alloxanthin	Cryptophytes
Diadinoxanthin	Dinoflagellates, diatoms, chrysophytes
Diatoxanthin	Diatoms, chrysophytes
Lutein- Zeaxanthin	Higher plants, chlorophytes, rhodophytes*, cyanobacteria
Echinenone	Total cyanobacteria
Canthaxanthin	Nostocales cyanobacteria
β-carotene	Total phototrophs

*In marine ecosystems, lutein-zeaxanthin also represents the Rhodophyta (Esteban et al., 2009).

Table 4. Factor loadings of the $\text{PCA}_{\text{pigments}}$ ran to explore potential associations in the community of primary producers as recorded by fossil pigment concentrations. Numbers in bold indicate pigments with highest factor loadings. Numbers in bold italics indicate pigments with moderate factor loadings.

	$\text{PC1}_{\text{pigments}}$	$\text{PC2}_{\text{pigments}}$
Variance explained	78%	13%
Diadinoxanthin	**0.85**	-0.07
Alloxanthin	0.14	-0.07
Diatoxanthin	-0.18	**0.55**
Lutein-zeaxanthin	***-0.23***	**0.49**
Canthaxanthin	***-0.21***	***-0.29***
Echinenone	***-0.37***	**-0.59**

Table 5. Factor loadings of the PCA$_{\text{environmental}}$ ran to decipher relationships between marker pigment composition and explicative variables. Numbers in bold indicate variables with the highest factor loadings and in bold. Numbers in bold and italics indicate variables with moderate factor loadings. Explicative variables are the Branched and Isoprenoid Tetraether (BIT) index -an index of the relative abundance of terrestrial organic matter versus marine input in marine sediments (Hopmans et al., 2004)-, Total Solar Irradiance (TSI, Vieira et al., 2011), index of North Atlantic Oscillation (NAO, Hurrell, 2003; Trouet et al., 2009; Olsen et al., 2012), Northern-Hemisphere Temperature (NHT, Kobashi et al., 2013), grain-size distribution, content of organic matter (OM), XRF-measured elements (Fe, Si, Ti, K, Ca, S, Cl and Br), carbon and nitrogen stable isotopes, chl-*a* and β-carotenes, and a pigment preservation index (chl-*a*/pheophytin *a*).

	PC1$_{\text{environmental}}$	PC2 $_{\text{environmental}}$
Variance explained	31%	26%
Diadinoxanthin	**-0.53**	-0.08
Alloxanthin	-0.01	0.00
Diatoxanthin	0.08	-0.10
Lutein-zeaxanthin	0.13	-0.10
Canthaxanthin	0.11	***0.13***
Echinenone	***0.22***	***0.14***
β-carotenes	***0.16***	***0.19***
chl-*a*	***-0.16***	***-0.19***
Mud	0.00	0.06
Fine sands	-0.02	***-0.17***
Medium sands	-0.01	***-0.18***
Coarse sands	0.02	**0.29**
Gravel	0.00	0.00
Si	-0.04	-0.02
S	-0.01	0.10
Br	0.00	0.08
Cl	0.00	**-0.32**
K	0.03	0.07
Ca	0.03	0.10
Ti	0.00	0.00
Fe	0.00	0.00
TSI	**-0.35**	0.11
NAO	0.01	-0.06
NHT	**-0.59**	0.16
BIT	0.06	**0.36**
$\delta^{13}C$	***-0.23***	-0.05
$\delta^{15}N$	-0.02	**0.37**
OM	***-0.17***	**0.43**
Preservation index	***-0.18***	**-0.21**

Highlights

- Fossil pigments can be used to reconstruct seagrass phototrophic community
- Phototrophic community composition was affected by local and global factors
- Global climate factors explained long-term changes in the dinoflagellates abundance
- Global warming may favour the development of dinoflagellates in seagrass meadows
- Phototrophic community changes might impact the seagrass ecosystem functioning

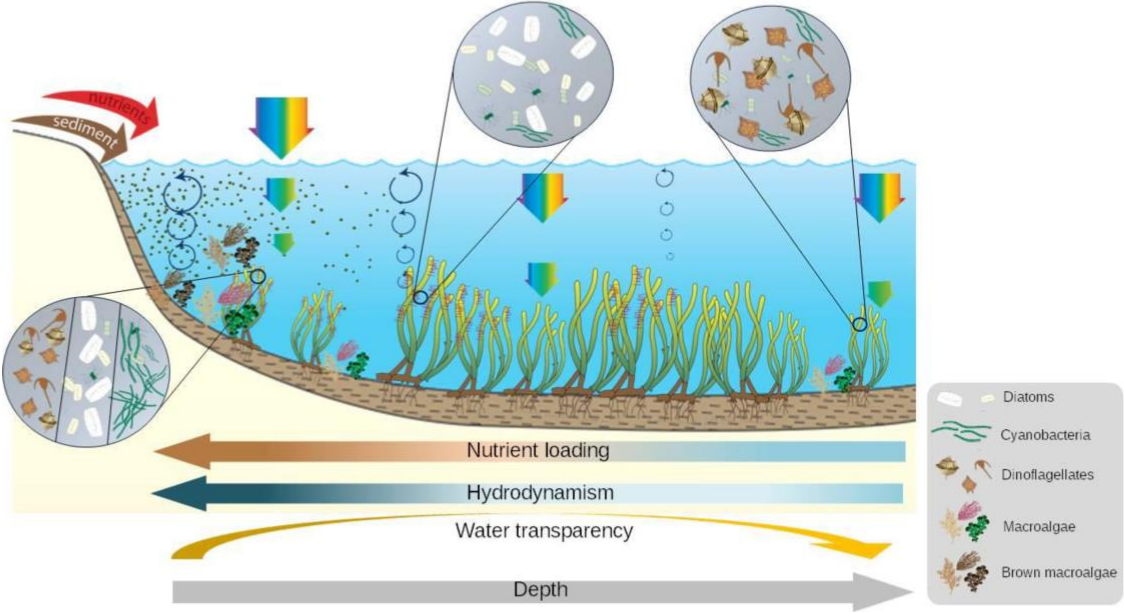
nutrients
sediment
Nutrient loading
Hydrodynamism
Water transparency
Depth
Diatoms
Cyanobacteria
Dinoflagellates
Macroalgae
Brown macroalgae

Figure 1

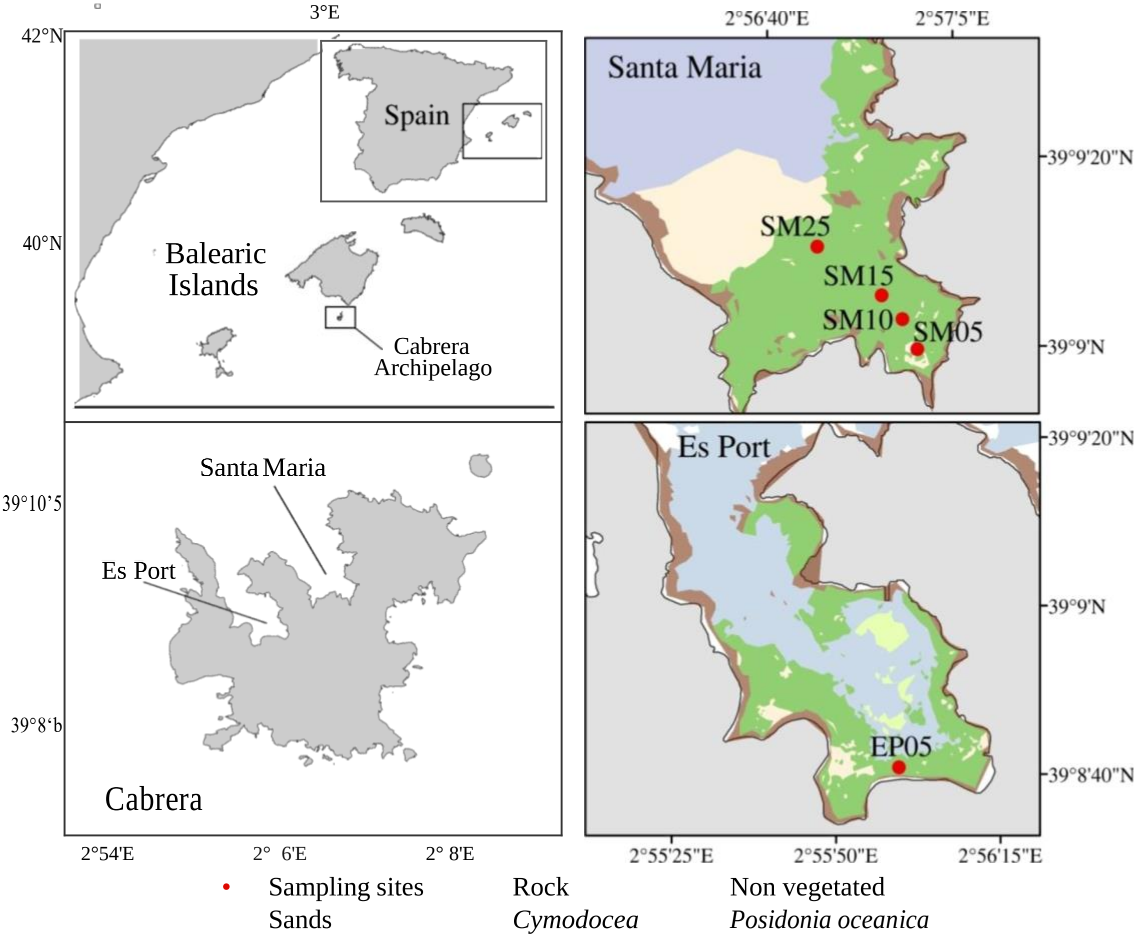
3°E
42°N
40°N
Spain
Balearic Islands
Cabrera Archipelago
Santa Maria
Es Port
Cabrera
39°10'5
39°8'b
2°54'E
2° 6'E
2° 8'E
2°56'40"E
2°57'5"E
39°9'20"N
39°9'N
SM25
SM15
SM10
SM05
Es Port
EP05
39°9'20"N
39°9'N
39°8'40"N
2°55'25"E
2°55'50"E
2°56'15"E
● Sampling sites
Sands
Rock
Cymodocea
Non vegetated
Posidonia oceanica

Figure 2

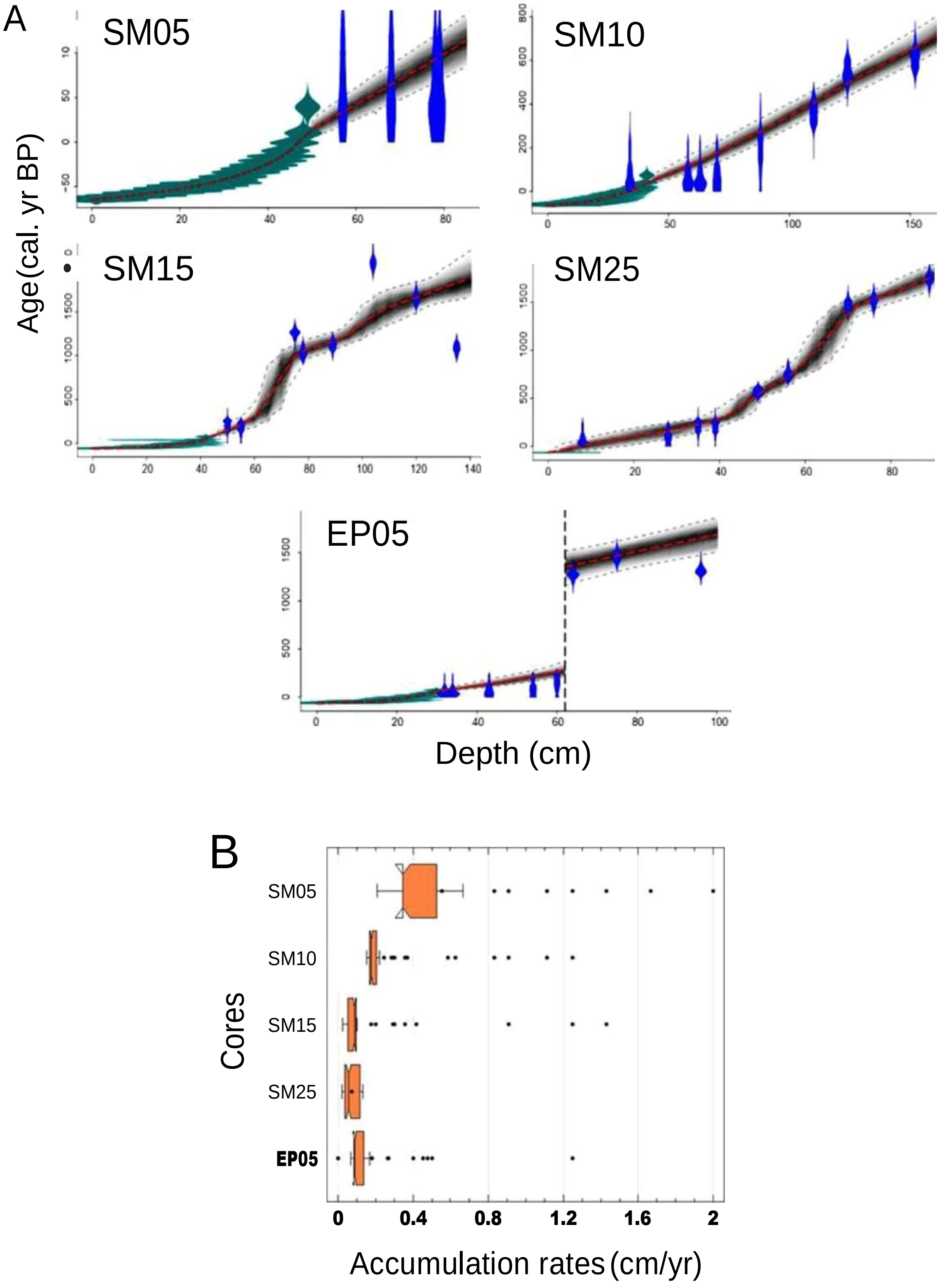
A
SM05
SM10
SM15
SM25
EP05
Age(cal. yr BP)
Depth (cm)
B
SM05
SM10
SM15
SM25
EP05
Cores
0
0.4
0.8
1.2
1.6
2
Accumulation rates (cm/yr)

Figure 3

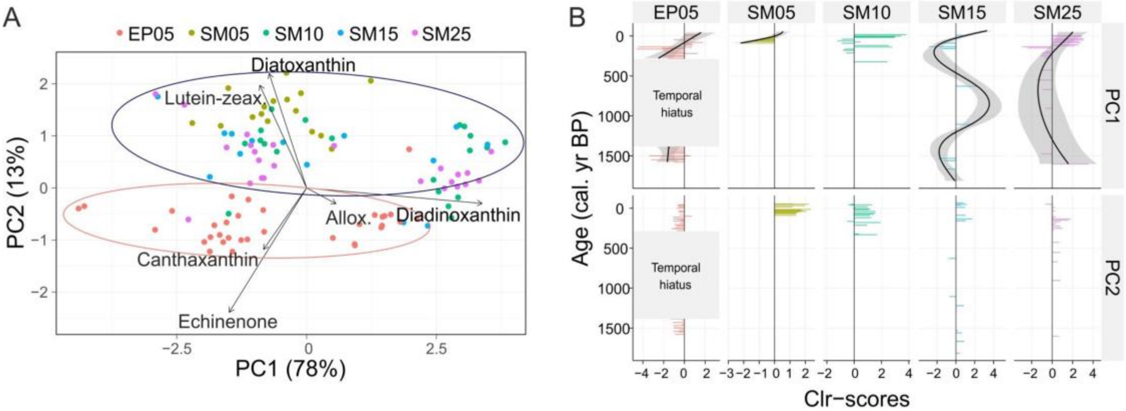
A
EP05
SM05
SM10
SM15
SM25
Diatoxanthin
Lutein-zeax.
Allox.
Diadinoxanthin
Canthaxanthin
Echinenone
PC2 (13%)
PC1 (78%)
2
1
0
−1
−2
−2.5
0
2.5
B
EP05
SM05
SM10
SM15
SM25
Temporal hiatus
Temporal hiatus
PC1
PC2
Age (cal. yr BP)
0
500
1000
1500
−4 −2 0 2
−3 −2 −1 0 1 2
−2 0 2 4
−2 0 2 4
−2 0 2 4
Clr−scores

Figure 4

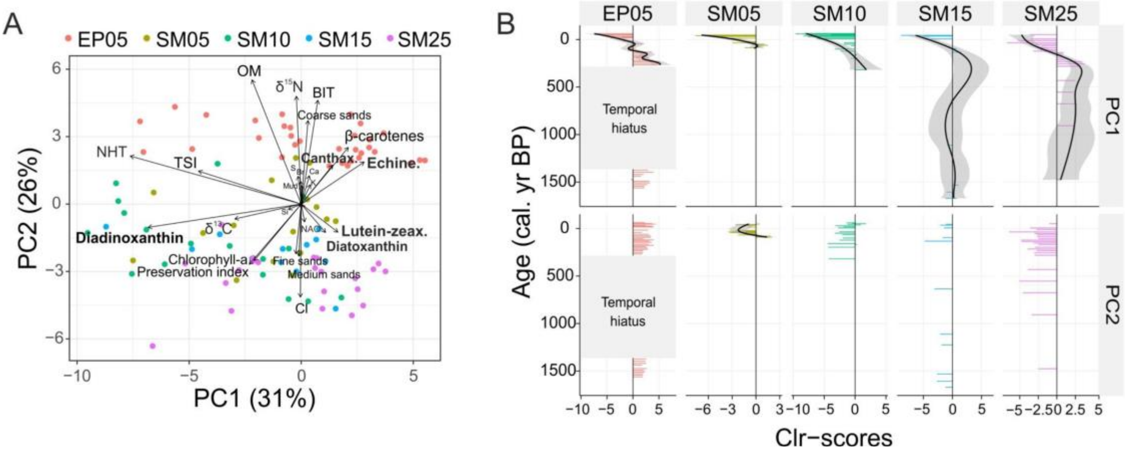
A
● EP05
● SM05
● SM10
● SM15
● SM25
OM
δ15N
BIT
Coarse sands
β-carotenes
NHT
TSI
Canthax.
Echine.
S
Br
Ca
Mud
Si
NAO
Lutein-zeax.
Diatoxanthin
δ13C
Diadinoxanthin
Chlorophyll-a
Fine sands
Preservation index
Medium sands
Cl
6
3
0
−3
−6
−10
−5
0
5
PC2 (26%)
PC1 (31%)
B
EP05
SM05
SM10
SM15
SM25
PC1
PC2
Temporal hiatus
Temporal hiatus
0
500
1000
1500
Age (cal. yr BP)
−10 −5 0 5
−6 −3 0 3
−10 −5 0 5
−5 0 5
−5 −2.5 0 2.5 5
Clr−scores

Figure 5

Figure 6

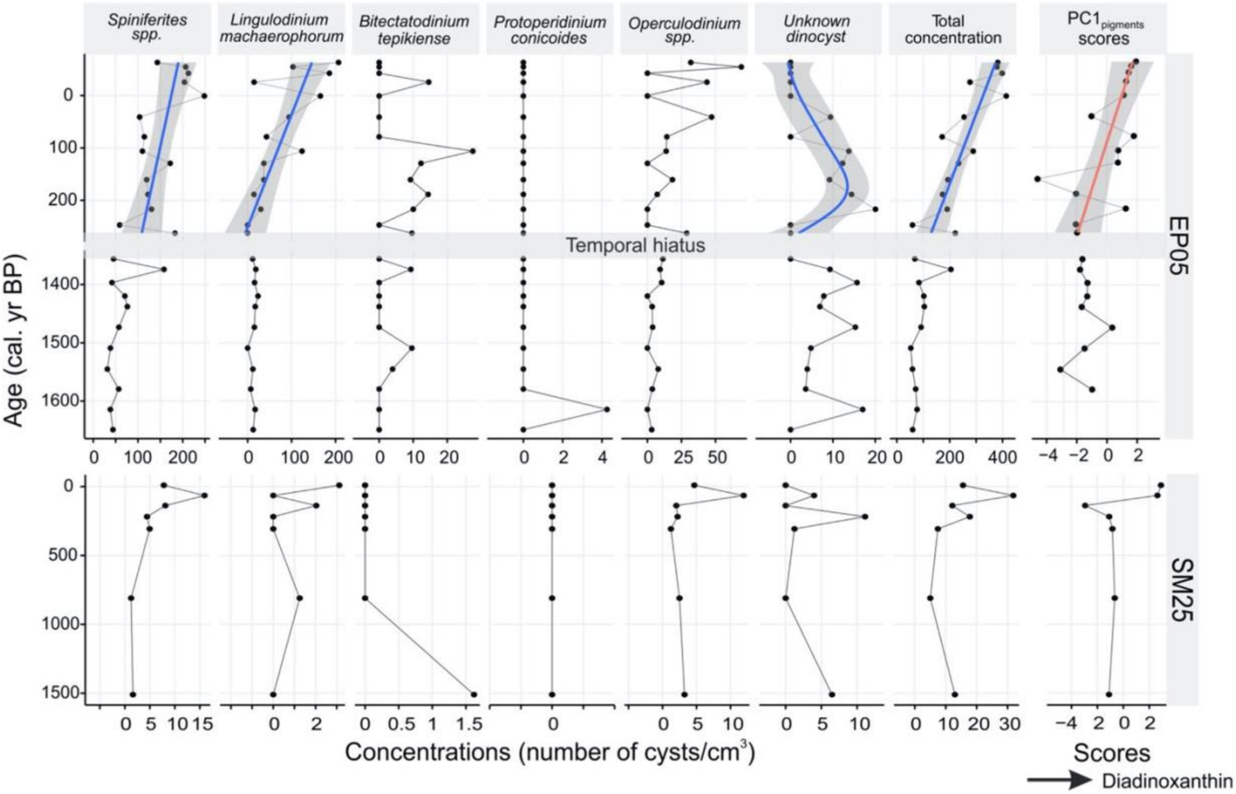

Spiniferites spp.
Lingulodinium machaerophorum
Bitectatodinium tepikiense
Protoperidinium conicoides
Operculodinium spp.
Unknown dinocyst
Total concentration
PC1$_{pigments}$ scores
Temporal hiatus
EP05
SM25
Age (cal. yr BP)
0
100
200
1400
1500
1600
500
1000
1500
0 100 200
0 100 200
0 10 20
0 2 4
0 25 50
0 10 20
0 200 400
−4 −2 0 2
0 5 10 15
0 2
0 0.5 1 1.5
0
0 5 10
0 5 10
0 10 20 30
−4 2 0 2
Concentrations (number of cysts/cm^3)
Scores
Diadinoxanthin

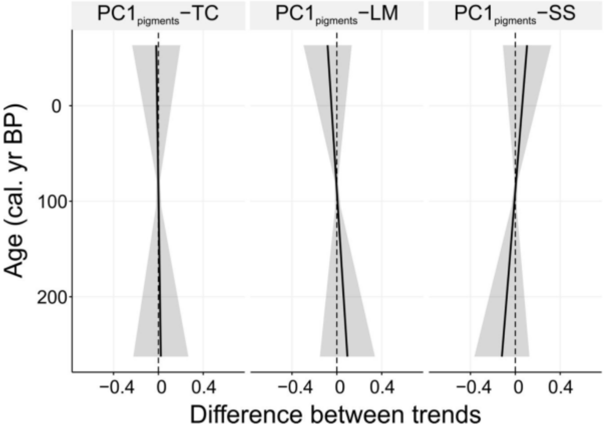
PC1pigments−TC
PC1pigments−LM
PC1pigments−SS
Age (cal. yr BP)
0
100
200
−0.4
0
0.4
Difference between trends

Figure 7